Published in final edited form as:
Small. 2011 November 18; 7(22): 3148–3152. doi:10.1002/smll.201101558.

CuInSe/ZnS Core/Shell NIR Quantum Dots for Biomedical Imaging

Jeaho Park,
Department of Materials Science and Engineering and Institute for Nanobiotechnology, Johns Hopkins University, 3400 N. Charles St., Baltimore, MD 21218, USA

Charlene Dvoracek,
Department of Materials Science and Engineering and Institute for Nanobiotechnology, Johns Hopkins University, 3400 N. Charles St., Baltimore, MD 21218, USA

Dr. Kwan Hyi Lee,
KIST Biomedical Research Institute, 5 Hwarangno 14-gil, Seongbuk-gu, Seoul 136-791, Korea

Justin F. Galloway,
Department of Materials Science and Engineering and Institute for Nanobiotechnology, Johns Hopkins University, 3400 N. Charles St., Baltimore, MD 21218, USA

Dr. Hyo-eun C. Bhang,
Department of Radiology, Johns Hopkins School of Medicine, Cancer Research Building, 1550 Orleans St., Baltimore, MD 21231, USA

Prof. Martin G. Pomper, and
Department of Radiology, Johns Hopkins School of Medicine, Cancer Research Building, 1550 Orleans St., Baltimore, MD 21231, USA

Prof. Peter C. Searson*
Department of Materials Science and Engineering and Institute for Nanobiotechnology, Johns Hopkins University, 3400 N. Charles St., Baltimore, MD 21218, USA

A current challenge in biomedical imaging is the synthesis of water-soluble quantum dots (QDs) with emission wavelengths in the near-IR, a high quantum yield, stability in water, and relatively small sizes. Ideally the synthesis should be relatively straightforward and not involve toxic elements. The optimum wavelength for in-vivo optical imaging, taking into account the absorbance from melanin in the epidermis, hemoglobin in blood, and water in tissue, is in the range of 700-900 nm.[1,2] To achieve emission in this optical window requires a QD with a bandgap of around 1.3–1.7 eV.[3] Semiconductor QDs that emit in the NIR—such as CdTe, PbS, InAs, InP—have been synthesized[4-8] and explored for biomedical imaging.[9-12] High quantum yield is important to optimize the signal-to-noise ratio for imaging, and stability in aqueous solutions is key to avoid aggregation and degradation during imaging. At the same time, it is thought that a hydrodynamic diameter less than about 15 nm is necessary to ensure renal clearance and to avoid accumulation in other organs.[13] In addition, due to concerns over toxicity if QDs are not cleared from the body, it is desirable to avoid elements such as cadmium, lead, and arsenic. Thus there remains a need for the development of QD systems that satisfy all of these requirements.

*searson@jhu.edu .

Supporting Information
Supporting Information is available from the Wiley Online Library or from the author.

Here we report the one-pot synthesis of $CuIn_xSe_y$/ZnS core/shell QDs with an emission wavelength $\lambda > 700$ nm. The 20% quantum yield of the core increases to as much as 60% after passivation with ZnS. After thiolation and lipid coating, the $CuIn_xSe_y$/ZnS/ dodecanthiol/lipid QDs are stable in water for about a week and maintain a high quantum yield. Fluorescence imaging in a mouse model is also shown, illustrating a uniform intensity that can be resolved without any image processing.

The $CuIn_xSe_y$ QDs were synthesized by reaction of CuI, InI_3, and bis(trimethylsilyl) selenide ($(TMS)_2Se$) in trioctylphosphine oxide (TOPO) and hexadecylamine (HDA). The Cu:In:Se precursor ratio was 1:4:14. After injection of the precursors at 270 °C over 6 s, the reaction was quenched by the injection of hexane. Large $CuInSe_2$ nanoparticles have been synthesized from Cu, In, and Se precursors in oleyamine (OA),[14,15] and $CuIn_xSe_y$ QDs have been synthesized from TOPO and OA.[16,17] However, we were not able to grow an effective passivation layer on $CuIn_xSe_y$ cores synthesized in these solvents. After investigating various combinations of the solvents TOPO, TOP, HDA, and OA, we found that the synthesis of $CuIn_xSe_y$ cores in TOPO and HDA with a mole ratio of 1:3 was optimum for one-pot passivation, high quantum yield, and stability in water (see the Supporting Information, (SI)).

Figure 1a shows the emission spectrum for $CuIn_xSe_y$ QD cores in chloroform. The emission peak is at 745 nm, well into the optical window for biomedical imaging. The full width at half maximum (FWHM) is about 133 nm. This synthesis is highly reproducible: the emission peak was 759 ± 20 nm and the FWHM was 133 ± 6 nm for 4 syntheses. The quantum yield of the cores was typically 20–30%. The absorbance spectrum for the $CuIn_xSe_y$ cores shows an absorption onset at about 800 nm, corresponding to the photoluminescence (PL) peak. Similar absorbance spectra have been reported for $CuIn_xSe_y$ cores synthesized from other solvent combinations.[16-18]

Figure 1b shows a representative energy-dispersive X-ray (EDS) spectrum for a $CuIn_xSe_y$ core along with a high-resolution transmission electron microscopy (TEM) image. The EDS spectrum confirms the presence of $CuIn_xSe_y$ with $x = 3.3$ and $y = 4.4$, close to the composition of the compound $CuIn_3Se_5$.[19] Detailed analysis of the particle size distribution was difficult due to the poor contrast, however, from analysis of TEM images we estimate an average size of 4.0 ± 0.1 nm (sample size $n = 39$). The relatively broad FWHM is ascribed to compositional variation since the reported bandgaps of $CuInSe_2$, $CuIn_3Se_5$, $CuIn_5Se_8$, are 1.04, 1.26, and 1.34 eV, respectively.

For most applications of QDs, the addition of a wide-bandgap shell is required to passivate surface states and increase the quantum yield. As shown below, the $CuIn_xSe_y$ cores have limited stability and hence the shell also serves to isolate the core from the environment. The emission peak at about 745 nm (Figure 1a) implies a bandgap of about 1.66 eV. This is significantly larger than the bandgap of 1.26 eV for $CuIn_3Se_5$ and implies significant confinement.[20] ZnS was selected as a passivation layer since it has a bulk bandgap of about 3.68 eV, and is commonly used to passivate II–VI QDs. In addition, the selection of ZnS allows us to avoid possible toxicity concerns by avoiding elements such as cadmium and arsenic. ZnS passivation of $CuIn_xSe_y$ QDs has been achieved after washing and resuspending the $CuIn_xSe_y$ cores in octadecene/OA prior to introducing the shell precursors and other reagents.[17] Here, successful passivation after injecting $(TMS)_2$ S and diethyl zinc directly into the suspension of $CuIn_xSe_y$ cores is demonstrated.

After the growth of the shell, the emission peak is slightly blue-shifted to 737 nm indicating a small decrease in the size of the core due to the formation of an alloy at the core/shell interface (Figure 1a). The FWHM is increased to 175 nm indicating a broader size

distribution resulting from the passivation process.[21-23] The core/shell synthesis produced an average emission peak of 741 ± 12 nm with a FWHM of 175 ± 9 nm for 4 syntheses. The quantum yield for the $CuIn_xSe_y$/ZnS QDs typically increased to 40–60%, confirming the importance of the passivation of surface states.

Figure 1c shows a representative EDS spectrum for a $CuIn_xSe_y$/ZnS QDs along with a high-resolution TEM image (see also the SI). The EDS spectrum (Figure 1c) confirms the presence of Zn and S in the $CuIn_xSe_y$/ZnS QDs. The average diameter of the core/shell QDs was 5.0 ± 0.2 nm (n = 72). The difference in average diameter between the cores and the core/shell QDs implies an average QD shell thickness of about 0.5 nm, in agreement with the expected value based on the concentration of precursors. X-ray powder diffraction spectra (Figure 1d) for the cores and core/shell QDs are consistent with the stannite crystal structure (space group I42m) for $CuIn_3Se_5$.[19]

The stability of the QDs was determined by measuring the time dependence of the quantum yield and PL. The quantum yield of the $CuIn_xSe_y$ cores in chloroform decreased rapidly after 1-2 days, indicating poor stability. Similar results were obtained for cores synthesized using the method reported by Allen et al.[16] The loss of stability was largely due to aggregation, as inferred from the fact that the emission peak remained constant at about 760 nm and the FWHM at about 130 nm.

The addition of the ZnS passivation layer resulted in an improvement in stability. The quantum yield in chloroform remained in the range 40–60% for 1–2 days but decreased to 10% after 4–5 days. The PL peak remained constant at about 730 nm and the FWHM remained at about 170 nm. Significant improvements in stability were obtained by replacing the TOPO/HDA coordinating ligands by dodecanethiol (DDT). The quantum yield for DDT-modified $CuIn_xSe_y$/ZnS QDs in chloroform remained high for 10–14 days, and decreased to 10% after 21 days (Figure 2a).

Lipid coating was used to transfer the $CuIn_xSe_y$/ZnS QDs to water.[24] Various combinations of single acyl chain lipid and double acyl chain lipids with polyethylene glycol (PEG) groups were tested. A lipid composition of 80% PEGylated lipid with 20% single acyl chain lipid gave the best results. These lipid coated QDs showed a quantum yield of about 50% in water and were stable for at least several days at room temperature (Figure 2b). After lipid coating, the average hydrodynamic diameter, measured by dynamic light scattering (DLS), was 15 nm (Figure 2c). As described above, the core/shell QDs are about 5 nm in diameter. Taking the DDT inner leaflet as 1 nm, the lipid outer leaflet as 2 nm, and the PEG radius of gyration as 2 nm, we expect the overall size to be about 15 nm, in excellent agreement with the measured particle size.

To explore the performance of the $CuIn_xSe_y$/ZnS QDs for biomedical imaging, fluorescence imaging was performed in mice after tail-vein injection. 230 pmol of lipid-coated QDs in 120 μL of saline were introduced by tail-vein injection. Fluorescence images were taken as a function of time post-injection (P.I.). Figure 3 shows fluorescence images recorded before injection, and at 5 min, 90 min, and 48 h P.I. Immediately after injection (Figure 3b) the fluorescence intensity increased relatively uniformly over the whole body of the mouse. Indeed, some of the larger blood vessels were easily detectable. The fluorescence intensity started to decay at 90 min P.I. (Figure 3c), and after 48 h had returned to the same level as before injection (Figure 3d). Very similar results were obtained for the other mice. There are no bright spots indicating aggregation or measurable accumulation in organs such as the liver or spleen, suggesting good clearance from the body (although this remains to be confirmed by quantitative analysis). Fluorescence images of the resected organs (see SI) show a similar dependence on time as the dorsal and ventral images; the fluorescence

increases to a maximum at about 30 min P.I., but then decreases to values close to background after 24 h.

The kinetics of circulation were analyzed quantitatively by determining the average intensity per pixel over the whole image (Figure 3e). The average intensity, *I*, remains constant for about 2 h P.I. and then decreases to the background level before injection after 48 h. By fitting the data to the function:

$$\frac{I(t) - I_{background}}{I_{max} - I_{background}} = \frac{1}{1+\exp\left(\frac{t-t_{1/2}}{\tau}\right)}$$

we obtain an average retention time $t_{1/2}$ of 268 ± 16 min and a clearance time τ of 74.5 ± 11.9 min.

These QDs are externally similar to the high density lipoprotein (HDL) particles in the body that carry cholesterol to the liver for clearance. HDL particles are lipid coated particles with diameter in the range from 10–15 nm and circulate freely in the body. As a result of these unique properties, modified natural HDL particles and biomimetic HDL particles have been explored as contrast agents for MRI.[25] Thus we hypothesize that the good circulation characteristics are due to the size and lipid coating.

In summary, we have demonstrated a one-pot synthesis of $CuIn_xSe_y$/ZnS QDs with emission in the NIR, high quantum yield, and good stability. The synthesis is relatively straightforward and reproducible, and avoids the use of elements such as Cd and As. We also have demonstrated that lipid coated $CuIn_xSe_y$/ZnS QDs are good candidates for in-vivo imaging.

Experimental Section

Cu/In Precursor Solution

Copper iodide (0.045 mmol, CuI, Alfa Aesar, puratonic, 99.999%) and indium iodide (0.18 mmol, InI_3, Alfa Aesar, anhydrous, 99.999%) were mixed with trioctylphosphine (3 mL TOP, Strem, 97%) in a glove box. The solution was stirred at 90 °C for several hours. The precursor solution was stored in the dark and was stable for up to two weeks.

Core Synthesis

Trioctylphosphine oxide (3.6 g, TOPO, Sigma Aldrich, tech. grade, 90%) and hexadecylamine (6 g, HDA, Sigma Aldrich, tech. grade, 90%) were added to a 100 mL 3-neck flask and heated to 100 °C in vacuum to form a transparent solution. The Cu/In precursor solution was injected into the reaction flask and vacuumed for at least 2 h. A more concentrated precursor solution can be used (3 times more concentrated) in order to decrease the amount of TOP. Reducing the amount of TOP makes the washing steps somewhat easier. The syringe and the flasks were wrapped with aluminum foil in order to minimize exposure to light. Next, the temperature was increased to 270 °C in Ar (Airgas, ultra high purity, grade 5) flow. Bis(trimethylsilyl) selenide (150 μL, $(TMS)_2Se$, Gelest) in TOP (0.5 mL) were mixed in a glove box and injected into the reaction flask. After 6 s, 4 mL hexane was injected to quench the reaction. The reaction mixture was then left to cool to 130 °C. While injecting hexane into the hot solution, a needle was placed in the septum to avoid a rapid increase in pressure in the flask.

ZnS Coating

Bis(trimethylsilyl)sulfide (227 μL, $(TMS)_2$ S, Sigma Aldrich, synthesis grade) and diethyl zinc (115 μL, Sigma Aldrich, 52.0 wt% Zn) were mixed with TOP (1 mL) in a glove box and injected into the suspension of $CuIn_xSe_y$ cores at 130 °C. Diethyl zinc is very reactive and should be handled with care. These precursor solutions were placed in a secondary container when transferring from the glove box to the hood to minimize exposure to air. Best results were obtained with fresh chemicals, typically within a month of opening. The amounts of Zn and S were calculated to achieve 3 monolayers (ML) ZnS on the $CuIn_xSe_y$ cores.[26] After injecting the precursors for the shell, the reaction mixture was cooled to 85 °C and the QDs annealed for 2 h. This annealing time was found to give the maximum quantum yield.

Dodecanethiol Functionalization

After annealing the $CuIn_xSe_y$/ZnS QDs for 2 h, dodecanethiol (1 mL, DDT, Sigma Aldrich, ≥ 98%) was injected into the QD suspension. Final solutions were poured into two 15 mL centrifugal tubes. Methanol and isopropyl alcohol (8:2 by volume) were added to the tubes until they were full. Using stronger solvents degraded the surface of QDs and resulted in aggregation. Too many washing steps (usually more than 3 times) also resulted in aggregation. The QD suspensions were centrifuged at 8000 rpm for 3 min. After centrifugation, the precipitate was redispersed in hexane and the same washing steps repeated at least twice. The final precipitate was re-dispersed in chloroform.

Water Solubilization

Deionised (DI) water (2 mL) was added to a 5 mL vial. A stirring rod was inserted into the vial to ensure good mixing. This vial was placed in a beaker containing glycerol maintained at a temperature of 110 °C using a hot plate. In a separate vial, polyethylene glycol oleyl ether (0.61 μmol, Brij93, Sigma Aldrich), 1,2-distearoyl-sn-glycero-3-phosphoethanolamine-*N*-[methoxy(polyethylene glycol)-2000] (2.43 μmol, DSPE-PEG2k, Avanti Polar Lipids), and 2.3×10^{14} QDs were mixed thoroughly. The amount of lipids corresponds to a 40-fold excess of with respect to the amount required for complete coverage of the QDs. A minimum 10-fold excess of lipids was necessary to achieve a good yield. This mixture was sonicated and then added drop-wise to the DI water at 100 °C under vigorous stirring for 2 min. The solution was then centrifuged at 4000 rpm for 3 min and the supernatant filtered through 200 nm syringe filter.

In-Vivo Imaging

Three mice were prepared for tail-vein injection. They were fed special food (TD97184,Teklad Purified Diet, Harlan) for a week prior to the experiment in order to eliminate autofluorescence from the food. 120 μL QD solution containing 60 μL of QDs and 60 μL of saline was injected into the tail vein and imaged using a Li-cor imaging system in the Small Animal Imaging Facility. The QD concentration was determined from absorbance measurements using an extinction coefficient of 3.1×10^6 cm^2 mol^{-1}, based on the number of moles of the solid phase. The extinction coefficient was determined from gravimetric measurements using a density of 3.49 g cm^{-3} for $CuIn_3Se_5$. Fluorescence images were taken at different time points. Procedures were conducted according to protocols approved by Johns Hopkins Animal Care and Use Committee.

Characterization

Photoluminescence (PL) measurements were obtained using a fluorometer (Fluorolog-3 fluorometer, Horiba Jobin Yvon). Absorbance spectra were obtained using a spectrophotometer (Cary 50 UV–vis). Suspensions of QDs in chloroform or in water were

placed in cuvettes with polished sides (Starna Cells, Inc.). TEM images and EDS data were obtained using a Philips EM 420 TEM and FEI Tecnai 12 TWIN. High resolution images were obtained using a Philips CM 300 FEG TEM. Samples for TEM were prepared by placing a drop of the QD suspension on a gold laceycarbon grid. The absolute QY was measured using an Absolute PL Quantum Yield Measurement System (Hamamatsu, C9920-02). Particle size distributions were measured using a Malvern Zetasizer. A Pearl Impulse Li-Cor system was used for small animal imaging. Pearl Impulse software and ImageJ were used for analysis of fluorescence images. XRD measurements were performed using a Phillip's X Pert 3040 with a Cu K_α source.

Supplementary Material

Refer to Web version on PubMed Central for supplementary material.

Acknowledgments

This work was supported in part by NIH (U54CA151838) and NSF (CHE-0905869).

References

[1]. Cheong WF, Prahl SA, Welch AJ. IEEE J. Quantum Elect. 1990; 26:2166.

[2]. Konig K. J. Microscopy. 2000; 200:83.

[3]. Medintz IL, Uyeda HT, Goldman ER, Mattoussi H. Nat. Mater. 2005; 4:435. [PubMed: 15928695]

[4]. Blackman B, Battaglia D, Peng XG. Chem. Mater. 2008; 20:4847.

[5]. Battaglia D, Peng XG. Nano Lett. 2002; 2:1027.

[6]. Chang JY, Wang SR, Yang CH. Nanotechnology. 2007:18.

[7]. Hines MA, Scholes GD. Adv. Mater. 2003; 15:1844.

[8]. Lin W, Fritz K, Guerin G, Bardajee GR, Hinds S, Sukhovatkin V, Sargent EH, Scholes GD, Winnik MA. Langmuir. 2008; 24:8215. [PubMed: 18597501]

[9]. Zimmer JP, Kim SW, Ohnishi S, Tanaka E, Frangioni JV, Bawendi MG. J. Am. Chem. Soc. 2006; 128:2526. [PubMed: 16492023]

[10]. Xie RG, Peng XG. Angew. Chem. Int. Ed. 2008; 47:7677.

[11]. Kim S, Lim YT, Soltesz EG, De Grand AM, Lee J, Nakayama A, Parker JA, Mihaljevic T, Laurence RG, Dor DM, Cohn LH, Bawendi MG, Frangioni JV. Nat. Biotechnol. 2004; 22:93. [PubMed: 14661026]

[12]. Hu R, Yong KT, Roy I, Ding H, Law WC, Cai HX, Zhang XH, Vathy LA, Bergey EJ, Prasad PN. Nanotechnology. 2010; 21:145150.

[13]. Choi HS, Liu W, Misra P, Tanaka E, Zimmer JP, Ipe BI, Bawendi MG, Frangioni JV. Nat. Biotechnol. 2007; 25:1165. [PubMed: 17891134]

[14]. Norako ME, Brutchey RL. Chem. Mater. 2010; 22:1613.

[15]. Guo Q, Kim SJ, Kar M, Shafarman WN, Birkmire RW, Stach EA, Agrawal R, Hillhouse HW. Nano Letters. 2008; 8:2982. [PubMed: 18672940]

[16]. Allen PM, Bawendi MG. J. Am. Chem. Soc. 2008; 130:9240. [PubMed: 18582061]

[17]. Cassette E, Pons T, Bouet C, Helle M, Bezdetnaya L, Marchal F, Dubertret B. Chem. Mater. 2010; 22:6117.

[18]. Nose K, Omata T, Otsuka-Yao-Matsuo S. J. Phys. Chem. C. 2009; 113:3455.

[19]. Paszkowicz W, Lewandowska R, Bacewicz R. J. Alloy Compd. 2004; 362:241.

[20]. Zhang SB, Wei SH, Zunger A, Katayama-Yoshida H. Phys. Rev. B. 1998; 57:9642.

[21]. Pesika NS, Stebe KJ, Searson PC. J. Phys. Chem. B. 2003; 107:10412.

[22]. Pesika NS, Stebe KJ, Searson PC. Adv. Mater. 2003; 15:1289.

[23]. Park J, Lee KH, Galloway JF, Searson PC. J. Phys. Chem. C. 2008; 112:17849.

[24]. Dubertret B, Skourides P, Norris DJ, Noireaux V, Brivanlou AH, Libchaber A. Science. 2002; 298:1759. [PubMed: 12459582]

[25]. Cormode DP, Jarzyna PA, Mulder WJM, Fayad ZA. Adv. Drug. Deliv. Rev. 2010; 62:329. [PubMed: 19900496]

[26]. Galloway JF, Park J, Lee KH, Wirtz D, Searson PC. Sci. Adv. Mater. 2009; 1:1.

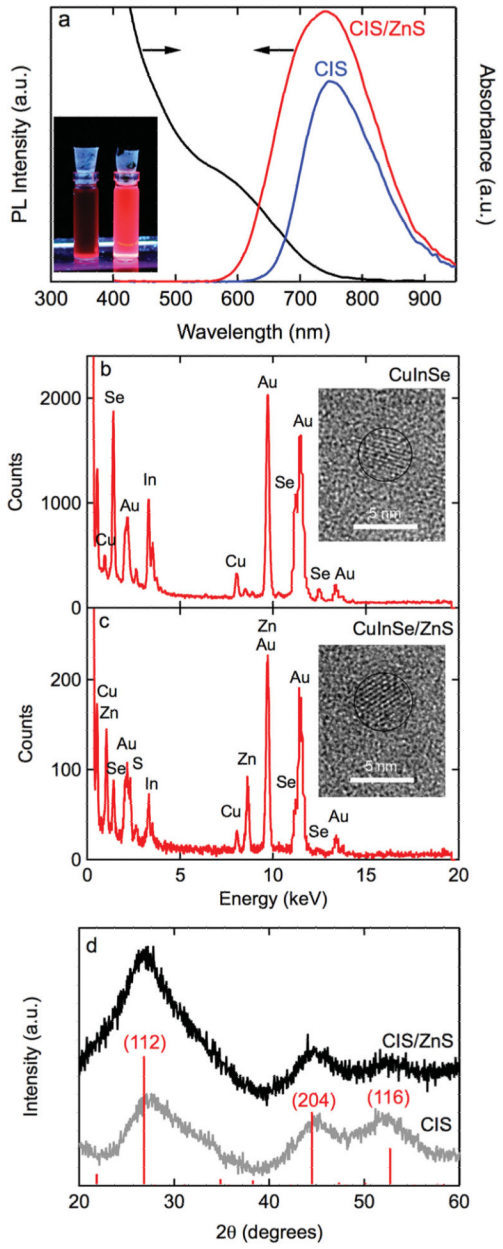

Figure 1.

a) Photoluminescence spectra for $CuIn_xSe_y$ (745 nm peak and 133 nm FWHM) and $CuIn_xSe_y$/ZnS QDs (737 nm peak with 175 nm FWHM), and an absorbance spectrum for $CuIn_xSe_y$/ZnS QDs. Inset shows a photograph of suspensions of $CuIn_xSe_y$ (left) and $CuIn_xSe_y$/ZnS (right) QDs in chloroform under UV excitation. The quantum yield increased from 20% to 50% after ZnS passivation. b) EDS spectrum QDs and high-resolution TEM image of a CuInSe QD. c) EDS spectrum and high-resolution TEM image for a $CuIn_xSe_y$/ZnS QD. The gold peaks in the spectra are from the TEM grid. The average diameter, obtained from analysis of TEM images, is 4.0 ± 0.13 nm for the $CuIn_xSe_y$ cores and 5.0 ± 0.17 nm for the $CuIn_xSe_y$/ZnS core/shell QDs. d) X-ray diffraction patterns for $CuIn_xSe_y$ and $CuIn_xSe_y$/ZnS QDs. The peak positions indicate the stannite form of $CuIn_3Se_5$ and their relative intensities are also shown.

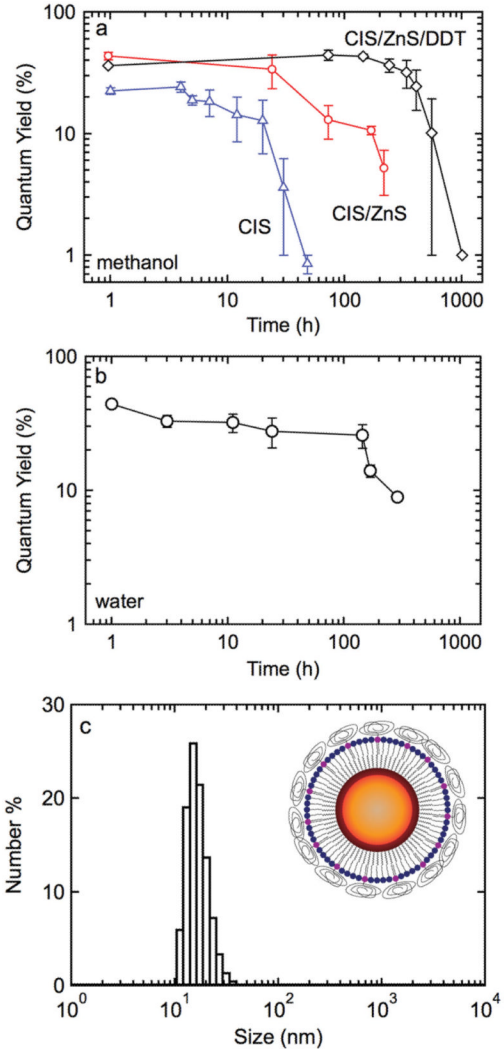

Figure 2.

a) Quantum yield over time for $CuIn_xSe_y$, $CuIn_xSe_y$/ZnS, and $CuIn_xSe_y$/ZnS/DDT QDs in chloroform. b) Quantum yield over time for $CuIn_xSe_y$/ZnS/DDT/lipid QDs in water. c) Size distribution of $CuIn_xSe_y$/ZnS/DDT/lipid QDs in water measured by DLS. The average diameter is 15 nm. The inset shows a schematic of the functionalized QDs.

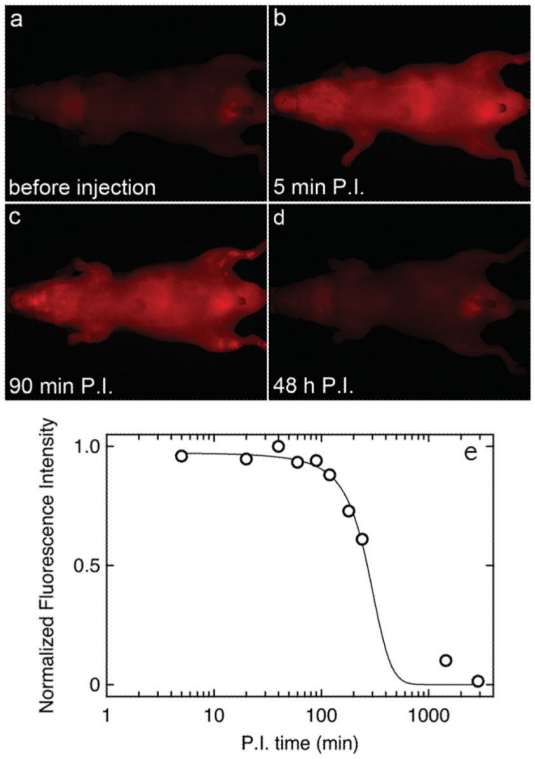

Figure 3.

Fluorescence images obtained from the ventral side of a mouse after tail-vein injection of 230 pmol QDs. a) Before tail-vein injection, b) 5 min post-injection, c) 90 min post-injection, and d) 48 h post-injection. e) Normalized average intensity per pixel (obtained from the fluorescence images) over time after injection.